Catalysis Today 149 (2010) 394–400

Contents lists available at ScienceDirect

Catalysis Today

journal homepage: www.elsevier.com/locate/cattod

Supported nickel catalysts with a controlled molecular architecture for the catalytic reformation of methane

Dirk Hufschmidt [a,*], L.F. Bobadilla [a], F. Romero-Sarria [a], M.A. Centeno [a], J.A. Odriozola [a], M. Montes [b], E. Falabella [c]

[a] Departamento de Química Inorgánica e Instituto de Ciencia de Materiales de Sevilla, Centro mixto, Universidad de Sevilla-CSIC, Avda. Américo Vespucio 49, 41092 Sevilla, Spain
[b] Grupo de Ingeniería Química, Dpto. Química Aplicada, Fac. Ciencias Químicas de San Sebastián, UPV/EHU, Paseo Manuel de Lardizábal 3, 20018 San Sebastián, Spain
[c] CENPES/Petrobrás, Centro de Pesquisas da Petrobrás, 21949-900 Rio de Janeiro, RJ, Brazil

ARTICLE INFO

Article history:
Available online 22 July 2009

Keywords:
Methane
Steam reforming
Nickel catalyst
Formation of carbon

ABSTRACT

In this work a lanthanum and nickel catalyst having perovskite structure, grown on a γ-alumina carrier, is being presented. The structure of the catalyst was confirmed by XRD. The behaviour of this material under the conditions of steam reforming has been studied and the influence of the temperature, the space velocity and the steam/carbon ratio on the conversion of methane and the product distribution in the process was determined. In all cases at higher temperatures conversions of more than 90% and high selectivities were achieved. The experiments to determine the stability of the catalyst demonstrated that no deactivation in experimental runs of more than 17 h occurred. Additionally a study of the catalyst after the reaction showed that only lowly structured carbonaceous species were formed on the catalyst surface, which is not expected to inhibit strongly the initial catalytic activity.

1. Introduction

In recent years the interest for synthesis gas for industrial purposes has grown steadily. Not only the production of the resulting hydrogen as energy carrier is of increasing importance [1], but also the use of synthesis gas for the production of highly valued products, like for example liquid hydrocarbons, proves to be a promising application for the future [2]. Besides the already widely spread application of synthesis gas for chemical synthesis, the use of the H_2/CO mixture also serve as a base for the Fischer-Tropsch (FT) process, resulting in the synthesis of high value mixtures of hydrocarbons [3]. Although being a process known for a long time [4], the FT process is experiencing a renaissance being a process capable of producing fuels from a large number of different carbon sources. Of the different sources for carbon methane, either coming from natural gas or being produced from biomass has currently the highest importance and will maintain it in the next years [5–8]. The GTL (gas-to-liquid) technology, a combination of the FT process with processes for the production of synthesis gas, possesses a high industrial potential and therefore has attracted the interest of many researchers [9–12]. Within the GTL process the production of synthesis gas from methane would represent ca. 60–70% of the total costs, which justifies the large number of studies devoted to methane reforming processes. Currently the most important processes for the production of synthesis gas from methane are steam reforming, partial oxidation with air or oxygen, dry reforming and autothermal reforming [6,13,14]. Each of these processes possess advantages and disadvantages, so that even being widely used and long time established still a large number of works are dedicated to the understanding and development of these processes. Recently, process intensification has led to the study of the steam reforming of natural gas in microchannel reactors in which heat necessary to drive the endothermic reforming reaction is supplied by catalytic oxidation proceeding in a series of channels parallel to those in which reforming occurs [14–16].

The interest of this work lies on the steam reforming process according to Eq. (1):

$$CH_4 + H_2O \rightarrow CO + 3H_2 \quad \Delta H^0_{298} = 206\,\mathrm{kJ\,mol^{-1}} \tag{1}$$

The steam reforming process provides the highest hydrogen yield among all possible reforming processes. The catalytic steam reforming of methane is a well established industrial process that has been described in considerable detail since the first detailed study by Neumann and Jacob in 1924. Many metals including nickel, cobalt, iron and the platinum group metals could catalyze the methane steam reforming to thermodynamic equilibrium [13,17]. Noble metals present clear advantages among these catalysts because their high activities and, most important, their

* Corresponding author. Tel.: +34 954460665.
E-mail address: dirk@icmse.csic.es (D. Hufschmidt).

0920-5861/$ – see front matter © 2009 Elsevier B.V. All rights reserved.
doi:10.1016/j.cattod.2009.06.002

high resistance to the formation of carbonaceous deposits on the catalyst surface preventing their deactivation [18,19]. Nevertheless, the elevated price of most noble metals has led to the use of nickel-based catalysts that are most cost-effective and are used industrially, although presenting sintering problems and especially exhibiting a high tendency to carburization leading to a rapid deactivation of the catalyst [20–22]. For these reasons, the current research on nickel catalysts is mainly focused on the minimisation of these disadvantages paying special attention to the role of the support.

The incorporation of nickel to perovskite type structures (ABO_3), which act as catalytic precursors, is one of the successful strategies for the preparation of nickel catalysts for the steam reforming of methane [23,24]. The reduction of these precursors results in well dispersed nickel particles, which increase the catalytic activity and the stability of the catalysts. When using lanthana as support for the nickel catalyst selectivities and conversions close to thermodynamic predictions with minimal carbon deposits are obtained [25], which suggests that lanthana contributes to distribute nickel and to facilitate carbon gasification. When lanthanum is used as a promoter of Ni/Al_2O_3 catalysts inhibits the phase transition to $NiAl_2O_4$ during calcination favouring the metal reducibility [26]. Additionally, as a strategy for the reduction of the poisoning of the catalyst by carbon deposits metals with a certain basic character can be added [26], in the case of lanthanum decoration of the nickel particles by La_2O_3 has been proposed as responsible for the reduction of carbon deposits during methane reforming [27,28]. In the present work a perovskite type $LaNiO_3$ catalyst supported on γ-Al_2O_3 has been prepared and studied in the steam reforming of methane. The preparation was carried out in two steps. In the first step a layer of La oxide was created over the core of a γ-alumina particle, which assumes the perovskite structure and additionally is adding a basic character to the catalyst. In a second step a layer of Ni in the form of Ni oxide was deposited on the first layer of La oxide. The first layer determines in this step the structure of the Ni oxide, in which the perovskite structure the first layer is repeated. The Ni oxide is then acting as a well-dispersed catalytic precursor, from which by reduction the elementary Ni^0 is formed.

The catalyst achieved by this method was characterised and tested in the reaction of the steam reforming of methane. The influence of a number of reaction variables, temperature, steam/carbon (S/C) ratio and space velocity on the reaction was investigated. Special attention was paid to catalyst stability.

2. Materials and methods

The preparation of the catalyst was carried out in two impregnation steps. In the first step a commercial γ-Al_2O_3 (Spheralite) with a BET-surface area of 100 m^2/g was impregnated with a $LaNO_3$ solution and further calcined at 900 °C for 4 h. By this procedure a material containing 15 mass% of La was obtained. This procedure ensures the formation of a $LaAlO_3$ monolayer with the perovskite structure on the γ-Al_2O_3 particles [29]. In the second step the impregnation was repeated employing a $NiNO_3$ solution. After the subsequent calcinations at 900 °C for 4 h the catalyst containing 15 mass% of Ni was obtained, here called Ni–La/γ-Al_2O_3.

The characterisation by XRD was carried out with a Siemens Kristalloflex D-501 diffractometer employing the Kα of copper (1.5418 Å) in an X-ray tube working at 36 kV and 26 mA.

The catalytic activity of the newly prepared material for the steam reforming of methane was tested in PID Eng&Tech Microactivity MAPGXM3 set-up, employing a Hastelloy C-276 tubular reactor (Autoclave Engineers) with an internal diameter of 9 mm. At the exit of the reactor the remaining water was removed from the gas flow by condensation and the gaseous components analysed by a GC Agilent 6890N, employing a GS-GasPro capillary column (60 m, ID 0.320 mm) and a Thermal Conductivity Detector (TCD) plus a Flame Ionisation Detector (FID), connected in series.

The amount of catalyst used for the experimental runs was varied in dependence of the designated space velocity. Prior to reaction the catalyst was reduced at 800 °C during 2 h in a stream of 20% H_2 in N_2 with a total flow of 100 mL/min. After this pretreatment the reactor containing the catalyst was flushed for at least 30 min in order to remove the traces of hydrogen from the system and to prevent the entry of oxidising species into the reactor before starting the experiment. The experimental runs were carried out with a constant flow of CH_4 of 100 mL/min and a flow of liquid water of 0.1–0.3 mL/min, corresponding to the designated steam/carbon ratio (S/C). From the gas stream leaving the reactor the remaining water was separated and the dry gas analysed by GC every 12 min.

3. Results and discussion

3.1. Catalyst characterisation

The catalyst and the intermediate precursors were characterised by X-ray Diffraction (XRD) (Fig. 1). The XRD pattern after the first impregnation step (La impregnation and calcination at 900 °C) corresponds to a mixture of $LaAlO_3$ perovskite and γ-alumina phases. The presence of the γ-Al_2O_3 phase is represented by the peaks at 39.2°, 45.8°, 60.4° and 66.6° among others (JCPDS-00-050-0741). The peaks at 23.39°, 33.22°, 41.25° and 54.13° can be attributed to the perovskite phase (JCPDS-01-085-1071). After nickel impregnation and further calcination diffraction lines assigned to the $NiAlO_3$ perovskite phase appear, the most significant peaks being at 23.20°, 33.15°, 41.03° and 59.5° among others (JCPDS-01-079-2450). The shift of the diffraction peaks means that a modification of the solid is produced after nickel addition, but the presence of perovskite is evident. The formation of surface monolayer of $LaAlO_3$ on γ-Al_2O_3 has been shown using different experimental set-up [29].

Molecular dynamic simulations allow explain this behaviour on the basis of the similarities between the lattice parameter of the alumina and the perovskite structures allowing for the growth of one structure on top of the other [23]. The projection of plane (1 1 0) indicates that the introduction of the perovskite cell is

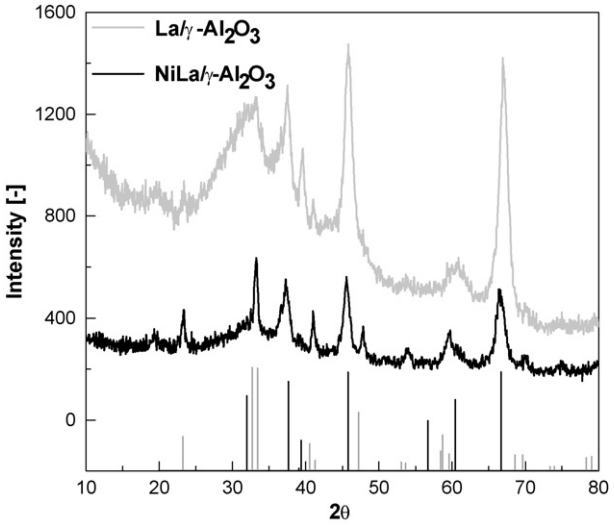

Fig. 1. XRD spectra of La/γ-Al_2O_3 and Ni–La/γ-Al_2O_3. The theoretical values based on the data base for γ-Al_2O_3 (JCPDS-00-050-0741, grey columns) and a perovskite phase (JCPDS-01-085-1071, black columns) are represented for comparison.

possible if the values of "*a*" and "*b*" are 5.2 Å. According to the data base (JCPDS-01-079-2450) in our case the lattice parameters are: $a = 5.4$ Å, $b = 5.4$ Å, $c = 13.1$ Å. Therefore, the growing of the perovskite lattice on the (1 1 0) plane of the γ-Al_2O_3 implies a modification of the "*a*" and "*b*" to 5.2 Å, which means a reduction of 3.7%. This value confirms that the growing of the structure on the initial cubic γ-alumina is possible. Following this argument it is possible to argue the formation of a $LaNiO_3$ perovskite layer on top of the $LaAlO_3$ previously formed layer because the similarities in structure and lattice parameters. Therefore, this method allows obtaining a catalytic precursor (perovskite) on a high surface area support having a high thermal stability (Al_2O_3), which results in a suitable material for the steam reforming of methane.

The measured BET-surface area of the commercial γ-Al_2O_3 is 100 m^2/g, which reduces to 77 m^2/g upon calcination at 900 °C. Lanthanum incorporation and subsequent calcination results in a decrease in the BET-surface area to 67 m^2/g. The further nickel impregnation and subsequent thermal treatment reduces again the BET-surface area that is now of 50 m^2/g. These data clearly show that this synthesis procedure leads to the intended La–Ni catalyst with perovskite structure on γ-Al_2O_3, maintaining a sufficient BET-surface area suitable for reforming reactions working at elevated temperatures. The apparent BET-surface area decrease with respect to the bare alumina support is explained on the basis of the weight increase as a result of the Ni and La additions.

It can be assumed that during the experiments carried out to determine the catalytic activity of this material no further change of BET-surface area and crystalline phase occurs due to the fact that all experiments have been performed at temperatures much below the calcination temperature of 900 °C. Also the stabilizing effect of the lanthanum present in the catalyst on the crystalline structure is well known throughout the literature [29].

3.2. Steam reforming of methane

The obtained catalyst (Ni–La/γ-Al_2O_3) has been tested in the steam reforming of methane reaction. The experiments were designed in order to establish the influence on methane conversion and product distribution of the following variables: temperature, space velocity and steam-to-carbon ratio (S/C). Moreover, the stability of the catalysts was studied by TPD and TPO analysis after reaction.

The influence of the temperature on the methane conversion and the distribution of the products have been studied at two different space velocities (120 000 and 240 000 mL g^{-1} h^{-1}) and constant S/C ratio of 1.24. The Figs. 2 and 3 show the relevant compositions in fraction of moles of the outlet gas streams on a dry basis. The conversion of methane is directly proportional to the molar fraction of methane still found in the outlet gas stream. The water still present in the gas stream was condensated, removed and not further quantified. The positive effect of the temperature is clear from these figures, it can be observed an increase of the conversion of methane with the temperature and consequently an increase of the quantities of H_2 and CO formed in the reaction.

At the highest space velocity tested, presented in Fig. 2, the diminution of methane stays relatively low for temperatures below 750 °C, at which it rapidly increases. This increase becomes more noticeable at higher temperatures, reaching a nearly equilibrium conversion at 850 °C. At the lowest space velocity tested, 120 000 mL g^{-1} h^{-1}, the methane diminished in the outlet gas stream continuously with the rise of temperature (Fig. 3).

Only CO, H_2 and CO_2 were detected at the outlet of the reactor. The evolution of the product distribution with the temperature is similar whatever the space velocity tested. In the low temperature range the observed H_2/CO ratio reaches much higher values than

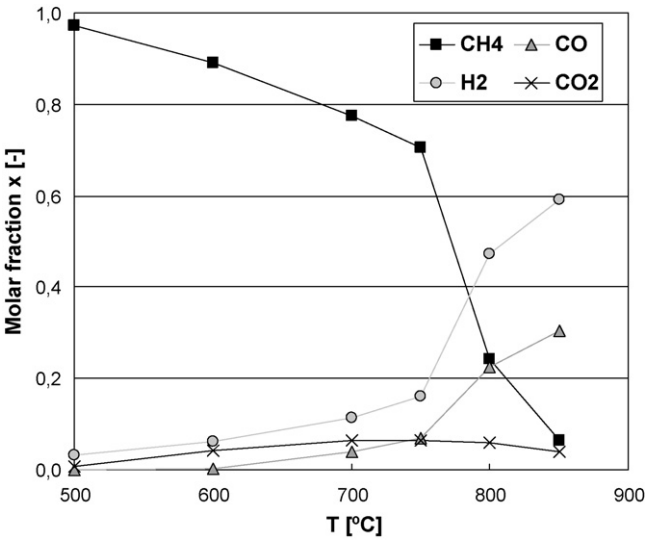

Fig. 2. Dependence of the catalytic activity of the temperature: composition of outlet gas stream (dry base). S/C = 1.24; GHSV 240 000 mL g^{-1} h^{-1}.

expected for the stoichiometric reaction, revealing the importance of the water gas shift reaction (WGS) in this temperature range. From ca. 700 °C the H_2/CO ratio values start to decrease approaching a value of 2 at 850 °C for a S/C ratio of 1.24. The measured CO_2 molar fraction shows a maximum at ca. 700 °C at 120 000 mL g^{-1} h^{-1} (750 °C at 240 000 mL g^{-1} h^{-1}). This observation together with the measured H_2/CO ratios indicates that in the high temperature range the exothermic WGS reaction is not any longer favourable, which results in the decrease in the CO_2 and H_2 molar fractions. In addition to this, the production of CO_2 by combustion of carbonaceous species formed on the catalyst may not be discarded since the high thermal stability of carbonate species formed on lanthana surfaces [30].

The S/C ratio strongly affects the product distribution. Two different S/C ratios, 1.24 and 3.72, keeping the space velocity equal to 120 000 mL g^{-1} h^{-1} have been investigated. A comparison of the product distributions for these S/C ratios and the obtained ones for the thermodynamic equilibrium in relation to the relation temperature is shown in Fig. 4.

In general, as it should be expected by considering the involved reactions, the increase in the H_2O/CH_4 ratio results in the increase

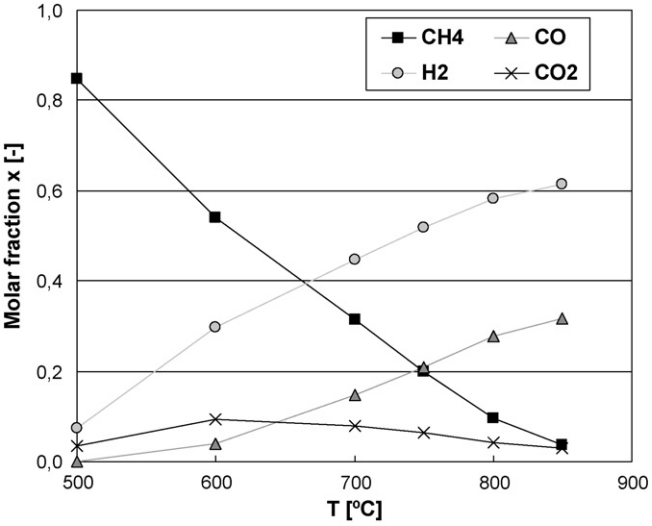

Fig. 3. Dependence of the catalytic activity of the temperature: composition of outlet gas stream (dry base). S/C = 1.24; GHSV 120 000 mL g^{-1} h^{-1}.

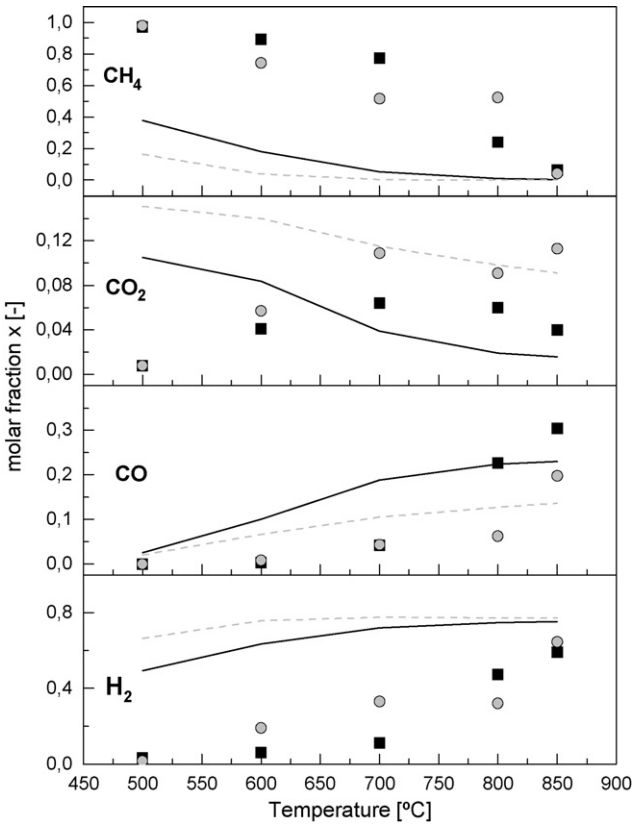

Fig. 4. Comparison of the product distributions for different S/C ratios and the obtained ones for the thermodynamic equilibrium. For S/C = 1.24: thermodynamic values (continuous lines), (■) experimental points. For S/C = 3.72, thermodynamic values (dashed lines), (◯) experimental points.

of methane conversion that almost reaches complete conversion at 850 °C whatever the S/C ratio employed. Also the hydrogen production increases in a similar manner as the methane is converted. The molar fractions of carbon oxides are varying significantly from those expected from the considered thermodynamic equilibria. While the carbon monoxide reaches higher experimental values than the thermodynamic ones above 800 °C, carbon dioxide clearly exceeds the thermodynamic values reaching a maximum of approx. 700 °C and diminishes reaching higher temperatures.

These data clearly indicate that the reaction taking place is much more complex than to assume exclusively the steam reforming of methane. Various side or follow-up reactions can be observed, the most important being the Water-Gas-Shift (WGS) reaction, the pyrolysis of methane and Boudouard equilibrium and others. These reactions were not considered in the thermodynamic calculation, which explains the variation of the experimentally determined values from the thermodynamically ones. Additionally it must be assumed that a number of reactions based on the interaction of the molecules inherent to the reaction and the special surface chemistry are taking place. These factors make it extremely difficult to carry out more precise thermodynamic calculations, which take all possible reactions in account.

The pyrolysis of methane and the Boudouard reaction are likely to form carbon deposited on the catalyst surface, thus deactivating it. The influence of these two reactions will be discussed later on. The WGS reaction clearly can be observed due to the high amounts of carbon dioxide, depending significantly on the temperature and the S/C ratio. Further on, in the presence of CO_2, the basic character of the lanthanum-containing layer will result in adsorbed carbonate species [31] that may further evolve to the formation of $La_2O_2CO_3$ as proposed by Tsipouriari and Verykios [27]. Moreover, hydrogen species produced at the metal particles may spill over the support surface giving rise to adsorbed formate species [32,33] that undergo a dehydration process for producing CO and adsorbed hydroxyl species. These processes are essentially similar to those proposed by Tsipouriari and Verykios [27] using Isotopic Tracing Techniques.

For the highest S/C ratio tested, the WGS reaction is favoured and the amount of CO_2 adsorbed is enhanced which justifies the higher molar fraction of CO_2 the higher the S/C ratio. At higher temperatures, this exothermic reaction is not favoured any more and the molar fraction of CO_2 decreases. Moreover, the catalyst activity for the steam reforming reaction increases and C formed by the dissociative adsorption of the methane molecule on the metallic nickel particle may react with the adsorbed CO_2 species forming carbon monoxide. This reaction could explain the molar fraction of CO above equilibrium at the highest temperatures tested.

The experiments carried out show clearly, the support plays a fundamental role in product distribution acting as a drain for carbon oxides and atomic carbon. At high temperatures it helps in maintaining a low H_2/CO ratio while oxidising carbon and thus preventing the catalyst deactivation.

3.3. Stability of the catalyst

The main reactions of the GTL process (reforming and Fischer-Tropsch) seem to be very suitable for the technology of microchannels since reforming is a very fast and endothermic reaction which requires very high heat flows and short contact times for the intensification thereof whereas Fischer-Tropsch synthesis is highly exothermal, requiring fine temperature control to improve its selectivity. Moreover, remote and offshore natural gas fields call for compact technologies to be located in space-restricted areas, such as on offshore platforms, FPSO vessels, or mobile skids. However, microchannel reactors can have some disadvantages when use in commercial practice is considered. The catalysts cannot be easily replaced upon deactivation and the small channels are submitted to the risk of blockage due to carbon formation [16]. Therefore, an important criterion for a newly developed catalyst intended to be used in an industrial GTL process carried out in microchannel reactors is long-term stability. By maintaining the Ni–La/γ-Al_2O_3 catalyst under reaction conditions over extended periods of time clues on the long-term stability are obtained. The gas flow compositions as a function of reaction time for two reaction conditions are plotted in Figs. 5 and 6. In all the conditions tested the gas flow composition at the reactor exit remains constant with time, moreover, no significant loss of catalytic activity occurs. The excellent stability observed in these experiments allows assuming a small formation of carbon taking place on the Ni–La/γ-Al_2O_3 catalyst. The carbon balance shown in Fig. 6 confirms this assumption, the number of carbon atoms measured at the exit and the entrance of the reactor is similar. The sum of carbon atoms at the exit of the reactor accounts for the $98.4 \pm 0.4\%$ of the feed carbon atoms at all the tested points for different times on stream. This behaviour is reproduced for all the reaction carried out using different space velocities, temperatures and S/C ratios (Table 1). The excellent carbon balance and gas flow composition clearly indicates a very small amount of deposited carbon and points to the long-term stability of the catalyst.

3.4. characterisation of carbon depositions on post-reaction catalysts

The deleterious effects of carbon on the catalyst activity, product distribution and microchannel blockage demand the study of the nature of the carbonaceous deposits formed in reforming

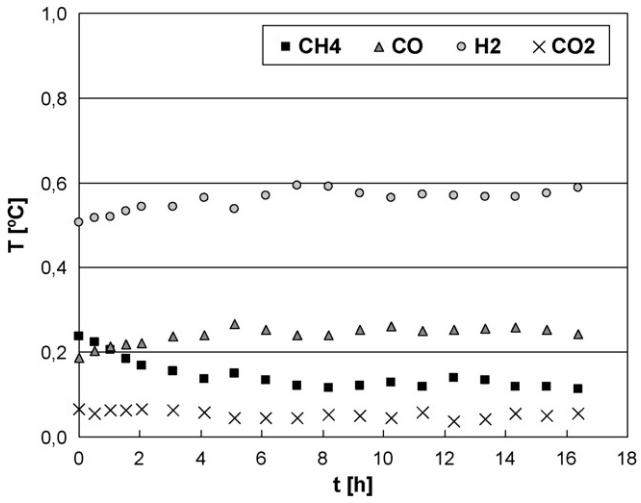

Fig. 5. Test for catalytic stability at 800 °C, S/C = 1.24; GHSV 240 000 mL g^{-1} h^{-1}.

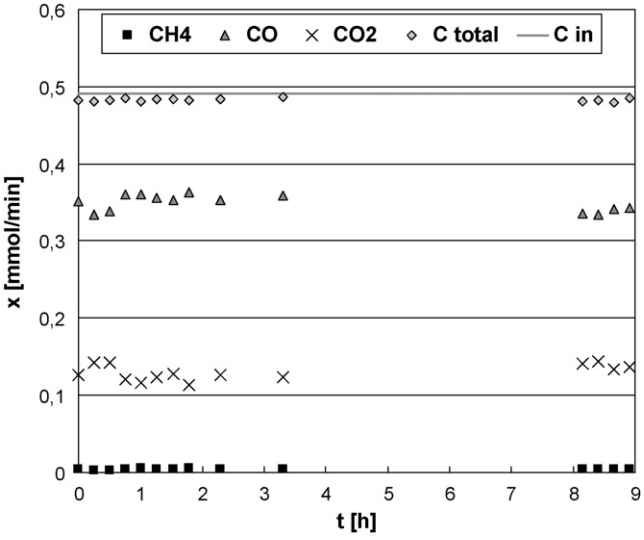

Fig. 6. Balance of carbonaceous species present in the gas stream in comparison to the amount of CH_4 entering the reactor; T = 800 °C, S/C = 3, GHSV 50 000 mL g^{-1} h^{-1}.

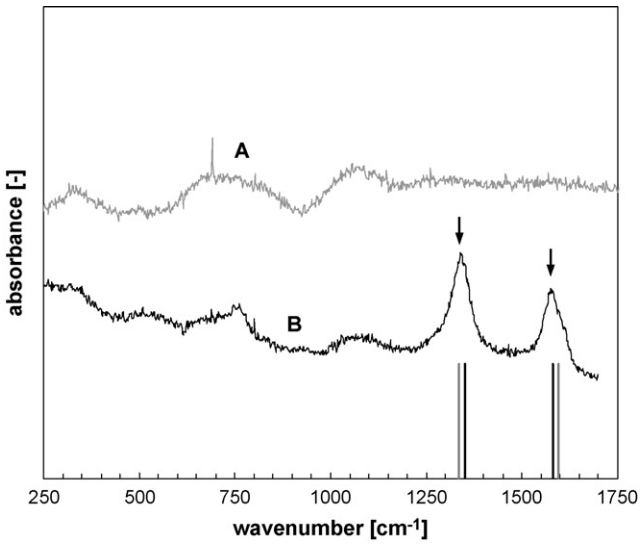

Fig. 7. Raman spectra of fresh Ni–La/γ-Al_2O_3 (A) and after 17.5 h of reaction (B). For comparison are given the D and G bands of graphite (black column) and carbon nanotubes (grey column).

reactions. Reacted samples were submitted to TPD and TPO experiments as well as studied by Laser Raman spectroscopy. The Raman spectra corresponding to the fresh and used catalyst are shown in Fig. 7. The spectrum of the used catalyst shows two bands at 1350 and 1580 cm^{-1}, which can be attributed to either graphite (D and G band at 1350 and 1580 cm^{-1}) or carbon nanotubes (D and G band at 1335 and 1595 cm^{-1}) [34,35]. However, the bandwidth, exact position and intensity of these bands strongly depend on the electronic structure of the carbon polymorph [36]. In the analysis of spent Ni/Al_2O_3 catalysts used in the steam reforming of propane, the presence of carbon structures were identified by TEM, these poorly graphitized structures resulted in Raman bands appearing at 1320 and 1597 cm^{-1} [37]. The Raman spectra of an Co/ZnO catalysts used for the steam reforming of methanol showed two bands at 1339–1345 and 1592–1597 cm^{-1} [38]. However, the presence of carbonaceous species cannot be completely assured because bands corresponding to carboxylic species appear at similar spectral positions. The stretching of the OCO group of adsorbed formate species on copper present two vibrational modes IR and Raman actives at 1330–1360 and 1550–1600 cm^{-1} [39]. Moreover, the hydrogenation of CO_2 on Rh/Ln_2O_3/Al_2O_3 catalysts results in the presence of adsorbed formate species characterized by the presence of bands at 1372 and 1592 cm^{-1} [32,33].

Considering the excess of water (oxidative conditions) in the reaction flow, the formation of carboxylic species cannot be discarded. The behaviour of the carbonaceous deposits depends on its nature. Adsorbed carboxylic species sit on the support sites and are probably not inhibiting the catalytic reaction since their decomposition to either CO and H_2O or CO_2 and H_2 at high temperatures is favoured [40,41], on the contrary, the graphite and carbon nanotube deposits lead to the irreversible deactivation of the catalyst by blocking the active sites or physically taking the Ni particles away from the support surface. Since no significant loss in the catalytic activity has been observed, the carbon deposits on the surface of the Ni–La/γ-Al_2O_3 catalyst do not seem to be formed by highly structured carbon polymorphs (graphene layers).

This seems to be contradictory to the reaction mechanism of methane reforming as is proposed in the literature [27,42]. It is assumed that methane decomposed in a dissociative adsorption on the catalyst surface, leading over CHX species to adsorbed carbon atoms, which either react with oxidative species or condensate to carbon nanotubes or to graphite structures. The former reaction is favoured by the presence of an excess of water and high temperatures while the latter one should occur at low S/C ratios and lower temperatures. The apparently low formation of carbon species and the fact that no deactivation of the catalyst was

Table 1
Carbon balance for the methane steam reforming process.

T [°C]	GHSV [mL g^{-1} h^{-1}]	S/C	C_{in} [mmol/min]	C_{out} [mmol/min]	$\Delta C = 100 \times \lvert C_{out} - C_{in}/C_{in} \rvert$
800	175 000	5	1.116	1.106	0.90
882	277 800	4.65	1.875	1.808	3.57
882	72 150	1.35	1.143	1.161	1.57

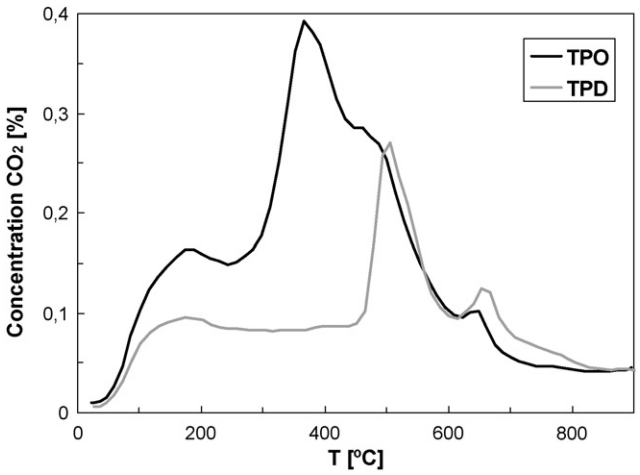

Fig. 8. TPO and TPD of a catalyst sample after a reaction of 2 h, GHSV = 48 000 mL g^{-1} h^{-1}, S/C = 1.24, T = 850 °C.

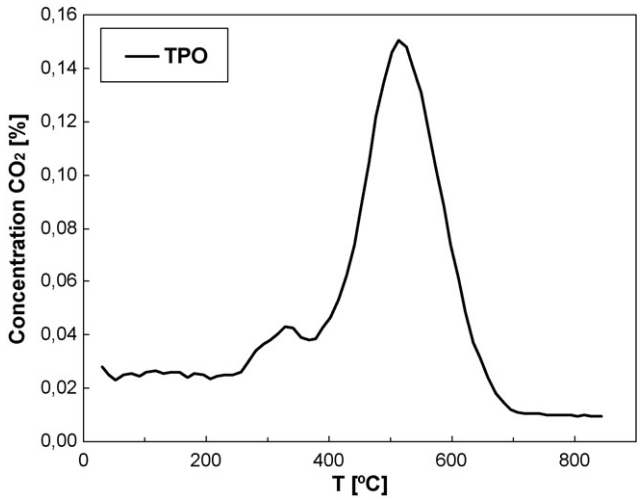

Fig. 9. TPO of a catalyst sample after a reaction of 17.5 h, GHSV = 240 000 mL g^{-1} h^{-1}, S/C = 1.24, T = 800 °C.

observed means that the latter process seems to be drastically inhibited. A possible cause could be the very fine dispersion of the Ni particles on the support, so that no higher C concentrations would be present, which could lead to well structured carbon deposits. Only unstructured carbon would be formed, which presents a very high reactivity towards oxidising species present in the reaction, mainly water, the CO_2 formed during the reaction and species containing oxygen present at the catalyst surface.

Temperature-programmed desorption or oxidation (TPD/TPO) were used to elucidate the nature of the carbonaceous deposits. While adsorbed carboxylate species decompose on increasing temperature in both, nitrogen and oxygen atmospheres, highly structured graphene deposits are only burnt off in oxygen containing atmospheres. In these temperature-programmed experiments a gas stream of either nitrogen or oxygen is passed through the catalyst and the temperature continuously increased up to 900 °C (10 °C/min). While the oxygen gas flow provokes the oxidation of carbonaceous species, the nitrogen flow results only in desorption or non-oxidative combustion of species adsorbed on the catalyst surface. In both cases, the formation of CO_2 is constantly monitored as a function of temperature. Fig. 8 shows the results of the TPD and TPO tests for the catalyst after 2 h of use (48 000 mL g^{-1} h^{-1}; 800 °C, S/C = 1.24). In the figure, maxima at ca.180, 500 and 650 °C are seen after the TPD experiment. A thermal decarboxylation process of the carbonaceous deposits must explain the CO_2 evolution under non-oxidising conditions (TPD). In the TPO experiment CO_2 maxima appear at 180, 380, 500 and 650 °C, as this experiment test both carboxylic and carbonaceous species (coke and graphene deposits) it must be concluded that coke species give rise to the maximum at 500 °C. The low temperatures at which the carbon deposits evolve suggest that these are lowly structured graphene layers, the ones responsible for the catalyst deactivation, are not formed during the reforming process.

These highly reactive carbon deposits together with molecules bearing carboxylic groups form the carbonaceous deposits on the surface of the used catalysts. The rate of formation of carbon nanotubes may be too small for detecting these species after a reaction period of 2 h, considering that a TPO analysis of the catalysts after 17.5 h in the reaction stream was carried out (Fig. 9). The TPO profile is now dominated by the peak at 500 °C (carboxylate decomposition) whose intensity has diminished with respect to the one obtained after 2 h in reaction (Fig. 8), the peak assigned to the carbonaceous deposits (350 °C) has decreased its intensity being now hardly visible. These observations indicate that even if formation of reactive carbonaceous species is possible in the conditions of reaction, the amount of these species decreases with reaction time, probably due to the high reactivity of these deposits towards water.

Additionally to this the presence of lanthana must be taken into account, which beneficial effect of suppressing formation of carbon was reported frequently. The basic surface acts as a drain for carbon oxide species probably through the formation of carboxylate species that further evolve to carbonates and finally to carbon dioxide at much higher temperatures. Further on, these carboxylates and carbonate can act in a similar manner as CO_2, to react with C atoms adsorbed on the catalyst surface or with lowly structured carbon, forming CO. This keeps the concentration of carbon atoms on the surface low and prevents from the formation of more structured carbon deposits, which would exhibit a much lower reactivity and would deactivated the catalyst. Generally, it could be said that the presence of high amounts of carboxylate and carbonates favours the oxidative pathway following the initial methane decomposition on the catalyst surface, leading to the formation of carbon oxides.

It should be noted that species like $La_2O_2CO_3$ or $La_2O(CO_3)_2$ are thermally stable at temperatures as high as 900 °C measured during the reaction, so that an accumulation should occur. As no deactivation of the Ni–La/γ-Al_2O_3 catalyst was detected under the reaction conditions, this accumulation is not poisoning the catalyst or is a very slow process. Also the thermal stability of these carbonates does not mean a chemical inertia against C atoms on the catalyst surface, so that these carbonates can contribute to the oxidation reaction, too.

4. Conclusions

A Ni–La catalyst with a perovskite structure over a surface of γ-Al_2O_3 has been successfully prepared. The catalytic activity of this catalyst in methane steam reforming was tested, and the influence of variables such as temperature, space velocity and S/C ratio was established. It was observed that:

High temperatures favour the reforming reaction.
High space velocities have a positive effect; especially at temperatures lower than 700 °C.
High water contents (high S/C) increase the hydrogen production and decrease the amount of CO.

Long time experiments evidenced the high catalytic stability of the Ni–La/γ-Al_2O_3 catalyst. A deeper analysis of the catalyst after reaction has let us conclude the absence of deactivation processes due to the formation of carbon whiskers.

Acknowledgements

This work has been realized in the framework of the scientific Project MAT2006-12386-C05-01. F. Romero-Sarria and L.F. Bobadilla acknowledge the contract of the program Ramón y Cajal and the fellowship provided by the Junta de Andalucía within the project POG-TEP-01965. The authors also like to thank Dr. L. Gandía and Dr. G. Arzamendi for the help with the thermodynamic calculations.

References

[1] J.R. Rostrup-Nielsen, Catal. Today 71 (2002) 243.
[2] K. Aasberg-Petersen, Ch. Stub Nielsen, I. Dybkjaer, Stud. Surf. Sci. Catal. 167 (2007) 243.
[3] L. Basini, Catal. Today 106 (2005) 34.
[4] F. Fisher, Berichte der Deutschen Chemischen Gesellschaft 59 (1926) 830.
[5] R.M. Navarro, M.A. Pea, J.L.G. Fierro, Chem. Rev. 107 (2007) 3952.
[6] J.R. Rostrup-Nielsen, J. Sehested, J.K. Norskov, Adv. Catal. 47 (2002) 65.
[7] M. Benito, S. García, P. Ferreira-Aparicio, L. García Serrano, L. Daza, J. Power Sources 169 (2007) 177.
[8] E.F. Sousa-Aguiar, L.G. Appel, C. Mota, Catal. Today 101 (2005) 3.
[9] L.C. Dong, S.A. Wei, S.Y. Tan, H.J. Zhang, Petr. Sci. 5 (2008) 388.
[10] Volkswagen AG, German Patent DE102007026643-A1.
[11] P. Jaramillo, W.M. Griffin, H.S. Matthews, Environ. Sci. Technol. 42 (2008) 7559.
[12] L.C. Almeida, O. González, O. Sanz, A. Paul, M.A. Centeno, J.A. Odriozola, M. Montes, Stud. Surf. Sci. Catal. 167 (2007) 79.
[13] D.L. Trimm, Z.I. Önsan, Catal. Rev. 43 (2001) 31.
[14] G. Arzamendi, P.M. Diéguez, M. Montes, J.A. Odriozola, E. Falabella Sousa-Aguiar, L.M. Gandía, Chem. Eng. J. (2009), doi:10.1016/j.cej.2009.01.035.
[15] A.Y. Tonkovich, B. Yang, S.T. Perry, S.P. Fitzgerald, Y. Wang, Catal. Today 120 (2007) 21.
[16] A.K. Avci, D.L. Trimm, M. Karakaya, Catal. Today (2009), doi:10.1016/j.cattod.2009.01.046.
[17] A.P.E. York, T. Xiao, M.L.H. Green, Catal. Rev. 49 (2007) 511.
[18] P.O. Graf, B.L. Mojet, J.G. van Ommen, L. Lefferts, Appl. Catal. A 332 (2007) 310.
[19] M.C.J. Bradford, M.A. Vannice, Catal. Rev. Sci. Eng. 41 (1999) 1.
[20] P. Vinten, J. Lefebvre, P. Finnie, Chem. Phys. Lett. 469 (2009) 293.
[21] N.V. Parizotto, K.O. Rocha, S. Damyanova, F.B. Passos, D. Zanchet, C.M.P. Marques, J.M.C. Bueno, Appl. Catal. A 330 (2007) 12.
[22] Z. Hou, J. Gao, J. Guo, D. Liang, H. Lou, X. Zheng, J. Catal. 250 (2007) 331.
[23] L.J. Alvárez, J. Fernández Sanz, M.C. Capitán, J.A. Odriozola, Catal. Lett. 21 (1993) 89.
[24] M.R. Goldwasser, M.E. Rivas, E. Pietri, M.J. Perez-Zurita, M.L. Cubeiro, L. Gingembre, L. Leclercq, G. Leclercq, Appl. Catal. 255 (2003) 45.
[25] V.A. Tsipouriari, Z. Zhang, X.E. Verykios, J. Catal. 179 (1998) 283.
[26] B.C. Enger, R. Lødeng, A. Holmen, Appl. Catal. A 346 (2008) 1.
[27] V.A. Tsipouriari, X.E. Verykios, J. Catal. 187 (1999) 85.
[28] A.N. Fatsikostas, D.I. Kondarides, X.E. Verykios, Catal. Today 75 (2002) 145.
[29] M.J. Capitán, M.A. Centeno, P. Malet, I. Carrizosa, J.A. Odriozola, A. Márquez, J.F. Sanz, J. Phys. Chem. 99 (1995) 4655.
[30] R. Alvero, J.A. Odriozola, J.M. Trillo, S. Bernal, J. Chem. Soc. Dalton Trans. (1984) 87.
[31] J.A. Odriozola, I. Carrizosa, R. Alvero, Stud. Surf. Sci. Catal. 48 (1989) 713.
[32] J.J. Benitez, R. Alvero, I. Carrizosa, J.A. Odriozola, Catal. Today 9 (1991) 53.
[33] J.J. Benitez, R. Alvero, M.J. Capitán, I. Carrizosa, J.A. Odriozola, Appl. Catal. 71 (1991) 219.
[34] J. Robertson, Mater. Sci. Eng. R 37 (2002) 129.
[35] M.S. Dresselhaus, G. Dresselhaus, P.C. Eklund, Science of Fullerenes and Carbon Nanotubes, Academic Press, London, 1996.
[36] A.C. Ferrari, Solid State Commun. 143 (2007) 47.
[37] L. Zhang, X. Wang, B. Tan, U.S. Ozkan, J. Mol. Catal. A 297 (2009) 26.
[38] J. Llorca, N. Homs, J. Sales, P. Ramírez de la Piscina, J. Catal. 209 (2002) 306.
[39] M. Pohl, A. Pieck, C. Hanewinkel, A. Otto, J. Raman Spectrosc. 27 (1996) 805.
[40] J.J. Benitez, I. Carrizosa, J.A. Odriozola, Appl. Spectrosc. 47 (1993) 1760.
[41] J.J. Benitez, I. Carrizosa, J.A. Odriozola, J. Chem. Soc. Faraday Trans. 89 (1993) 3307.
[42] G. Sierra-Gallego, C. Batiot-Dupeyrat, J. Barrault, F. Mondragón, Ind. Eng. Chem. Res. 47 (2008) 9272.